arXiv:1109.0481v1 [cond-mat.mes-hall] 2 Sep 2011

Spin-resolved noise in transport through T-shaped double quantum dots

JunYan Luo,[1, *] Yu Shen,[1] Xiao–Ling He,[1] Shiping Ruan,[1] and Changrong Wang[1]
[1] *School of Science, Zhejiang University of Science and Technology, Hangzhou 310023, China*

We investigate fluctuations of spin-dependent current through T-shaped double quantum dots connected with ferromagnetic electrodes. Based on the spin-resolved master equation approach, we are able to analyze individual self or mutual spin correlation shot noises for different electrode magnetization configurations (parallel and antiparallel alignments). Owing to the modulation of the interdot coupling, as well as the interplay between the Coulomb interaction and spin polarization in the electrodes, a number of remarkable noise behaviors, such as super-Poissonian self spin correlation, positive or negative mutual spin correlation noises, are revealed. The associated underlying mechanisms responsible for these results are discussed.

PACS numbers: 72.25.-b, 72.70.+m, 73.23.Hk, 73.23.-b

I. INTRODUCTION

Being stimulated by the efficient control of electron spin as well as its remarkably long coherence time, a growing interest has emerged in spin-dependent transport through open quantum dot (QD) systems. These spin-based nano-devices exhibit not only the fundamental physics but also promising applications in the technologies of spintronics and quantum information[1–6]. A number of different mechanisms, such as ferromagnetic resonance in a ferromagnetic-normal-metal, electron-spin resonance in a QD-based system with sizable Zeeman splitting, etc. have been proposed to produce spin-polarized current[7–11]. In this situation, transport is governed not only by the charge flow, but also, more importantly, by the spin dynamics.

However, study of the spin current alone does not provide enough spin-related information. A more effective method would be the measurement of spin current fluctuations. Complementary to the shot noise of charge current, which measures fluctuations of charge transport and can provides unique information beyond the average charge current[12, 13], the spin-resolved noise, due to the discreteness of the spin carrier, is more useful to describe spin correlation because the electronic wave packet with opposite spins is uninfluenced by the Pauli exclusion principle and only reflects unambiguous information about the interaction. The spin-resolved noise is shown to be capable of probing attractive or repulsive interactions in mesoscopic systems and measuring the spin relaxation time[14]. Through measurement of the spin current correlations, the spin unit of the quasiparticle in transport can be determined[15]. For a quantum dot strongly coupled to a cavity field, the fluctuations of the spin current exhibit a clear signature of the discrete nature of the photon states[16]. In the strong Coulomb blockade regime, shot noise of magnetically pumped spin current through a QD is found closely related to the magnetic Rabi frequency and spin decoherence[17].

In this work we study spin-dependent transport through a system of two coupled quantum dots connected with ferromagnetic (FM) electrodes, as schematically shown in Fig. 1. The coupled dots is arranged in special parallel geometry (so–called T-shaped double dots), where only QD1 is connected to the electrodes[18–20]. This type of setup itself is of particular interest, since it can be mapped onto resonant tunneling through an impurity inside the quantum well when the conducting level is tunnel coupled to other localized level, which indeed has been investigated in a recent experiment[21, 22]. By employing a spin-resolved master equation approach, which is obtained by proper extension to include spin degrees of freedom[23–26], we are able to analyze individual self or mutual spin correlations, as well as the fluctuations of the total spin and charge currents for different (parallel and antiparallel) magnetization configurations of electrodes. The special arrangement of the QD2 in side-connection to QD1 provides an additional path of electron propagation. Together with the interplay between the Coulomb correlation and the spin polarization of the FM electrodes, a number of remarkable behaviors in spin-resolved noises will be revealed. Furthermore, these unique noise features can serve as additional tools in experiments for revealing the intrinsic interdot coupling, as well as the involving Coulomb interactions.

II. MODEL DESCRIPTION

The system under study is schematically shown in Fig. 1. The QD1 is connected to the left and right FM electrodes whereas the QD2 is side-connected to the QD1. The entire Hamiltonian assumes

$$\hat{H} = \hat{H}_{\rm B} + \hat{H}_{\rm S} + \hat{H}'. \tag{1}$$

Here $\hat{H}_{\rm B} = \sum_{\alpha={\rm L,R}} \sum_{k,\sigma} \varepsilon_{\alpha k} c^\dagger_{\alpha k\sigma} c_{\alpha k\sigma}$ describes the left and right electrodes, which are magnetically polarized. $c_{\alpha k\sigma}$ ($c^\dagger_{\alpha k\sigma}$) is the electron annihilation (creation) operator of the electrode $\alpha =$ L or R, with spin $\sigma = \uparrow$ or $\downarrow$. The FM electrodes are characterized by the spin-dependent

---

[*] Electronic address: jyluo@zust.edu.cn

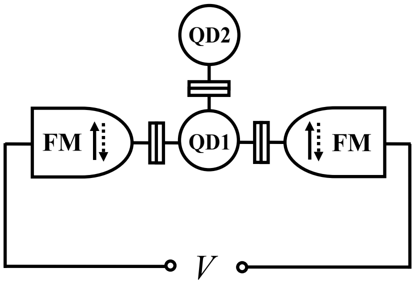

FIG. 1: Schematic setup for spin-dependent transport through T-shaped double quantum dots connected with ferromagnetic electrodes.

density of states $g_{\alpha\sigma}(\omega)$, which is assumed to be energy independent i.e. $g_{\alpha\sigma}(\omega) = g_{\alpha\sigma}$. Real ferromagnets will have a structured density of states[27]. This fact, however, will only modify details of the results and not the main physical picture. The degree of spin polarization in the FM electrodes is simply determined by the parameter $p_\alpha = (g_{\alpha\uparrow} - g_{\alpha\downarrow})/(g_{\alpha\uparrow} + g_{\alpha\downarrow})$, which satisfies $-1 \leqslant p_\alpha \leqslant 1$.

The second Hamiltonian is for the coupled dots:

$$\begin{aligned}\hat{H}_{\mathrm{S}} &= \sum_{l=1,2}\left[\sum_{\sigma=\uparrow,\downarrow} E_l \hat{n}_{l\sigma} + U_0 \hat{n}_{l\uparrow}\hat{n}_{l\downarrow}\right] + U'\hat{n}_1\hat{n}_2 \\ &\quad + \Omega\sum_\sigma (d^\dagger_{1\sigma} d_{2\sigma} + d^\dagger_{2\sigma} d_{1\sigma}). \qquad (2)\end{aligned}$$

Here $\hat{n}_{l\sigma} = d^\dagger_{l\sigma} d_{l\sigma}$ and $\hat{n}_l = \sum_\sigma \hat{n}_{l\sigma}$, with $d_{l\sigma}$ ($d^\dagger_{l\sigma}$) the electron annihilation (creation) operator in QD1 (l=1) or QD2 (l=2), and spin $\sigma =\uparrow$ or $\downarrow$. Each dot only has one spin-degenerate level in transport. U_0 and U' are respectively the intradot and interdot Coulomb interactions; and Ω is the coupling strength between the two dots. Here, we consider the two dots in the double-dot Coulomb blockade (DDCB) regime, such that at most one electron can resides in the double dots. Experimentally, the above condition can be achieved by appropriately adjusting the applied bias voltage with respect to the intradot and interdot charging energies[25, 28].

The third Hamiltonian describes the coupling of the QD1 to the electrodes, in terms of $\hat{H}' = \sum_{\alpha k\sigma}\left(t_{\alpha k} c^\dagger_{\alpha k\sigma} d_{1\sigma} + \mathrm{H.c.}\right)$. Note that, due to spin polarization of the electrodes, the tunnel coupling strength would become spin-dependent, i.e., with $\Gamma_{\alpha\uparrow} = \frac{1}{2}(1 + p_\alpha)\Gamma_\alpha$ differing from $\Gamma_{\alpha\downarrow} = \frac{1}{2}(1 - p_\alpha)\Gamma_\alpha$, where $\Gamma_\alpha = 2\pi\sum_k |t_{\alpha k}|^2 \delta(\varepsilon_{\alpha k} - \omega)$ is the total coupling strength regardless the spin orientation.

III. FORMALISM

In this section we outline the master equation approach for the calculation of the spin-resolved shot noise. The main point is to obtain the equation of motion for the *conditional* reduced density matrix of the central quantum dots, which is conditioned not only on the transmitted electron numbers, but also on their spins.

A. Spin-resolved master equation

To achieve the description of spin-dependent transport, we first extend the "n"-resolved quantum master equation[23–26] to include the spin degrees of freedom. Let us start with the reduced density matrix, defined as $\rho(t) \equiv \mathrm{Tr}_{\mathrm{B}}[\rho_{\mathrm{T}}(t)]$, i.e. tracing over the electrode states from the total density matrix. Assuming the tunneling Hamiltonian $\hat{H}'$ is weak, the second-order cumulant expansion leads to the master equation[29],

$$\dot{\rho}(t) = -i\mathcal{L}\rho(t) - \int_0^\infty d\tau \langle \mathcal{L}'(t)\mathcal{G}(t,\tau)\mathcal{L}'(\tau)\mathcal{G}^\dagger(t,\tau)\rangle\rho(t), \qquad (3)$$

where the Liouvillian superoperators are defined as $\mathcal{L}A \equiv [\hat{H}_{\mathrm{S}}, A]$, $\mathcal{L}'A \equiv [\hat{H}', A]$, and $\mathcal{G}(t,\tau)A \equiv G(t,\tau)AG^\dagger(t,\tau)$, with $G(t,\tau)$ the usual propagator associated with the system Hamiltonian $\hat{H}_{\mathrm{S}}$.

To condition the master equation on the spin of transmitted electrons[23–25], we decompose the entire Hilbert space B of the left and right electrodes into the sum of the subspaces, $\mathrm{B}_{\mathrm{L}}^{(n_{\mathrm{L}\uparrow}, n_{\mathrm{L}\downarrow})} \otimes \mathrm{B}_{\mathrm{R}}^{(n_{\mathrm{R}\uparrow}, n_{\mathrm{R}\downarrow})}$, where $n_{\alpha\sigma}$ is the number of electrons with spin-σ arrived at the electrode α (α=L or R). Partial tracing over electrode states in each subspace leads to the spin-resolved quantum master equation for the reduced density matrix[26],

$$\begin{aligned}\dot{\rho}^{\binom{n_{\mathrm{L}\uparrow},\, n_{\mathrm{R}\uparrow}}{n_{\mathrm{L}\downarrow},\, n_{\mathrm{R}\downarrow}}} &= -i\mathcal{L}\rho^{\binom{n_{\mathrm{L}\uparrow},\, n_{\mathrm{R}\uparrow}}{n_{\mathrm{L}\downarrow},\, n_{\mathrm{R}\downarrow}}} - \frac{1}{2}\Bigg\{\sum_{\alpha\sigma}\left[d^\dagger_{1\sigma} A^{(-)}_{\alpha\sigma}\rho^{\binom{n_{\mathrm{L}\uparrow},\, n_{\mathrm{R}\uparrow}}{n_{\mathrm{L}\downarrow},\, n_{\mathrm{R}\downarrow}}} + \rho^{\binom{n_{\mathrm{L}\uparrow},\, n_{\mathrm{R}\uparrow}}{n_{\mathrm{L}\downarrow},\, n_{\mathrm{R}\downarrow}}} A^{(+)}_{\alpha\sigma} d^\dagger_{1\sigma}\right] \\ &\quad - \Bigg[d^\dagger_{1\uparrow}\rho^{\binom{n_{\mathrm{L}\uparrow}+1,\, n_{\mathrm{R}\uparrow}}{n_{\mathrm{L}\downarrow},\, n_{\mathrm{R}\downarrow}}} A^{(+)}_{\mathrm{L}\uparrow} + d^\dagger_{1\downarrow}\rho^{\binom{n_{\mathrm{L}\uparrow},\, n_{\mathrm{R}\uparrow}}{n_{\mathrm{L}\downarrow}+1,\, n_{\mathrm{R}\downarrow}}} A^{(+)}_{\mathrm{L}\downarrow} + A^{(-)}_{\mathrm{L}\uparrow}\rho^{\binom{n_{\mathrm{L}\uparrow}-1,\, n_{\mathrm{R}\uparrow}}{n_{\mathrm{L}\downarrow},\, n_{\mathrm{R}\downarrow}}} d^\dagger_{1\uparrow} \\ &\quad + A^{(-)}_{\mathrm{L}\downarrow}\rho^{\binom{n_{\mathrm{L}\uparrow},\, n_{\mathrm{R}\uparrow}}{n_{\mathrm{L}\downarrow}-1,\, n_{\mathrm{R}\downarrow}}} d^\dagger_{1\downarrow} + d^\dagger_{1\uparrow}\rho^{\binom{n_{\mathrm{L}\uparrow},\, n_{\mathrm{R}\uparrow}+1}{n_{\mathrm{L}\downarrow},\, n_{\mathrm{R}\downarrow}}} A^{(+)}_{\mathrm{R}\uparrow} + d^\dagger_{1\downarrow}\rho^{\binom{n_{\mathrm{L}\uparrow},\, n_{\mathrm{R}\uparrow}}{n_{\mathrm{L}\downarrow},\, n_{\mathrm{R}\downarrow}+1}} A^{(+)}_{\mathrm{R}\downarrow} \\ &\quad + A^{(-)}_{\mathrm{R}\uparrow}\rho^{\binom{n_{\mathrm{L}\uparrow},\, n_{\mathrm{R}\uparrow}-1}{n_{\mathrm{L}\downarrow},\, n_{\mathrm{R}\downarrow}}} d^\dagger_{1\uparrow} + A^{(-)}_{\mathrm{R}\downarrow}\rho^{\binom{n_{\mathrm{L}\uparrow},\, n_{\mathrm{R}\uparrow}}{n_{\mathrm{L}\downarrow},\, n_{\mathrm{R}\downarrow}-1}} d^\dagger_{1\downarrow}\Bigg] + \mathrm{H.c.}\Bigg\}. \qquad (4)\end{aligned}$$

TABLE I: Spin-dependent currents, as well as the total charge and spin currents for different magnetic configurations: (i) parallel case ($p_{\rm L}=p_{\rm R}=p$) and (ii) antiparallel case ($p_{\rm L}=-p_{\rm R}=p$).

Currents	$\bar{I}^{\uparrow}_{\rm L/R}$	$\bar{I}^{\downarrow}_{\rm L/R}$	$\bar{I}^{\rm ch}_{\rm L/R}$	$\bar{I}^{\rm sp}_{\rm L/R}$
$p_{\rm L}=p_{\rm R}=p$	$\frac{(1+p)}{2}\frac{e\Gamma_{\rm L}\Gamma_{\rm R}}{4\Gamma_{\rm L}+\Gamma_{\rm R}}$	$\frac{(1-p)}{2}\frac{e\Gamma_{\rm L}\Gamma_{\rm R}}{4\Gamma_{\rm L}+\Gamma_{\rm R}}$	$\frac{e\Gamma_{\rm L}\Gamma_{\rm R}}{4\Gamma_{\rm L}+\Gamma_{\rm R}}$	$p\frac{e\Gamma_{\rm L}\Gamma_{\rm R}}{4\Gamma_{\rm L}+\Gamma_{\rm R}}$
$p_{\rm L}=-p_{\rm R}=p$	$\frac{(1-p)(1+p)^2e\Gamma_{\rm L}\Gamma_{\rm R}}{8(1+p^2)\Gamma_{\rm L}+2(1-p^2)\Gamma_{\rm R}}$	$\frac{(1+p)(1-p)^2e\Gamma_{\rm L}\Gamma_{\rm R}}{8(1+p^2)\Gamma_{\rm L}+2(1-p^2)\Gamma_{\rm R}}$	$\frac{(1-p^2)e\Gamma_{\rm L}\Gamma_{\rm R}}{4(1+p^2)\Gamma_{\rm L}+(1-p^2)\Gamma_{\rm R}}$	$\frac{p(1-p^2)e\Gamma_{\rm L}\Gamma_{\rm R}}{4(1+p^2)\Gamma_{\rm L}+(1-p^2)\Gamma_{\rm R}}$

Here, $A^{(+)}_{\alpha\sigma} \equiv \sum_{\sigma'} C^{(+)}_{\alpha\sigma'\sigma}(+\mathcal{L})d_{1\sigma'}$ and $A^{(-)}_{\alpha\sigma} \equiv \sum_{\sigma'} C^{(-)}_{\alpha\sigma\sigma'}(-\mathcal{L})d_{1\sigma'}$, with $C^{(\pm)}_{\alpha\sigma\sigma'}(\pm\mathcal{L}) = \int dt C^{(\pm)}_{\alpha\sigma\sigma'}(t)e^{\pm i\mathcal{L}t}$. The involved bath correlation functions are defined as $C^{(+)}_{\alpha\sigma\sigma'}(t-\tau) \equiv \langle f^{\dagger}_{\alpha\sigma}(t) f_{\alpha\sigma'}(\tau)\rangle$ and $C^{(-)}_{\alpha\sigma\sigma'}(t-\tau) \equiv \langle f_{\alpha\sigma}(t) f^{\dagger}_{\alpha\sigma'}(\tau)\rangle$, with $f_{\alpha\sigma} = \sum_k t_{\alpha\sigma} c_{\alpha k\sigma}$ and $\langle\cdots\rangle \equiv {\rm Tr}_{\rm B}[(\cdots)\rho_{\rm B}]$ standing for the usual meaning of thermal bath average.

B. Spin-dependent currents

With the knowledge of the above conditional state, the joint probability distribution function is obtained as $P[\binom{n_{\rm L\uparrow},\, n_{\rm R\uparrow}}{n_{\rm L\downarrow},\, n_{\rm R\downarrow}}, t] \equiv {\rm Tr}\rho^{\binom{n_{\rm L\uparrow},\, n_{\rm R\uparrow}}{n_{\rm L\downarrow},\, n_{\rm R\downarrow}}}$, where ${\rm Tr}(\cdots)$ denotes the trace over the system states. It allows us to evaluate the spin-σ dependent current through the junction α

$$I^{\sigma}_{\alpha} = e\frac{d}{dt}\sum_{n_{\rm L\uparrow},n_{\rm L\downarrow}}\sum_{n_{\rm R\uparrow},n_{\rm R\downarrow}} n_{\alpha\sigma} P\left[\binom{n_{\rm L\uparrow},\, n_{\rm R\uparrow}}{n_{\rm L\downarrow},\, n_{\rm R\downarrow}}, t\right] = e{\rm Tr}\dot{N}^{\sigma}_{\alpha}, \tag{5}$$

with $N^{\sigma}_{\alpha} \equiv \sum_{n_{\rm L\uparrow},n_{\rm L\downarrow},n_{\rm R\uparrow},n_{\rm R\downarrow}} n_{\alpha\sigma}\rho^{\binom{n_{\rm L\uparrow},\, n_{\rm R\uparrow}}{n_{\rm L\downarrow},\, n_{\rm R\downarrow}}}$. Based on Eq. (4), it can be calculated via its equation of motion

$$\begin{aligned}\frac{d}{dt}N^{\sigma}_{\alpha} &= -i\mathcal{L}N^{\sigma}_{\alpha} - \frac{1}{2}\Bigg\{\sum_{\alpha'\sigma'}\Big[d^{\dagger}_{1\sigma'}, A^{(-)}_{\alpha'\sigma'}N^{\sigma}_{\alpha} - N^{\sigma}_{\alpha}A^{(+)}_{\alpha'\sigma'}\Big] \\ &\quad + \Big[d^{\dagger}_{1\sigma}\rho(t)A^{(+)}_{\alpha\sigma} - A^{(-)}_{\alpha\sigma}\rho(t)d^{\dagger}_{1\sigma}\Big] + {\rm H.c.}\Bigg\}. \end{aligned}\tag{6}$$

Straightforwardly, it leads to

$$I^{\sigma}_{\alpha} = \frac{1}{2}e{\rm Tr}\left\{\left[d^{\dagger}_{1\sigma}A^{(-)}_{\alpha\sigma} - A^{(+)}_{\alpha\sigma}d^{\dagger}_{1\sigma}\right]\rho(t) + {\rm H.c.}\right\}, \tag{7}$$

where $\rho(t)$ is the unconditional density matrix that satisfies Eq. (3), or

$$\dot{\rho}(t) = -i\mathcal{L}\rho(t) - \frac{1}{2}\sum_{\alpha\sigma}\left\{\left[d^{\dagger}_{1\sigma}, A^{(-)}_{\alpha\sigma}\rho(t) - \rho(t)A^{(+)}_{\alpha\sigma}\right] + {\rm H.c.}\right\}. \tag{8}$$

C. Spin-dependent noises

Note that the total charge and spin currents through junction α are $I^{\rm ch}_{\alpha} = I^{\uparrow}_{\alpha} + I^{\downarrow}_{\alpha}$ and $I^{\rm sp}_{\alpha} = I^{\uparrow}_{\alpha} - I^{\downarrow}_{\alpha}$. The total charge current noise and spin current noise can then be expressed as

$$S^{\rm ch}_{\alpha\alpha'} = S^{\uparrow\uparrow}_{\alpha\alpha'} + S^{\downarrow\downarrow}_{\alpha\alpha'} + S^{\uparrow\downarrow}_{\alpha\alpha'} + S^{\downarrow\uparrow}_{\alpha\alpha'}, \tag{9a}$$

$$S^{\rm sp}_{\alpha\alpha'} = S^{\uparrow\uparrow}_{\alpha\alpha'} + S^{\downarrow\downarrow}_{\alpha\alpha'} - S^{\uparrow\downarrow}_{\alpha\alpha'} - S^{\downarrow\uparrow}_{\alpha\alpha'}, \tag{9b}$$

where the individual spin-resolved noise spectrum is defined as $S^{\sigma\sigma'}_{\alpha\alpha'}(\omega) \equiv \int_{-\infty}^{\infty} dt \cos(\omega t)\langle\{\Delta I^{\sigma}_{\alpha}(t), \Delta I^{\sigma'}_{\alpha'}(0)\}\rangle$, with $\Delta I^{\sigma}_{\alpha}(t) \equiv I^{\sigma}_{\alpha}(t) - \bar{I}^{\sigma}_{\alpha}$. In the following, fluctuation between the same or opposite spin currents is referred to as self or mutual spin correlation shot noise, respectively. Based on the MacDonald's formula[30–32], it follows that

$$S^{\sigma\sigma'}_{\alpha\alpha'}(\omega) = 2\omega\int_0^{\infty} dt \sin(\omega t)\frac{d}{dt}\big[M^{\sigma\sigma'}_{\alpha\alpha'}(t) - \bar{I}^{\sigma}_{\alpha}\bar{I}^{\sigma'}_{\alpha'}t^2\big], \tag{10}$$

where $\bar{I}^{\sigma}_{\alpha}$ is the stationary current obtained from Eq. (8), and $M^{\sigma\sigma'}_{\alpha\alpha'}(t) \equiv e^2\sum_{n_{\rm L\uparrow},n_{\rm L\downarrow},n_{\rm R\uparrow},n_{\rm R\downarrow}} n_{\alpha\sigma}n_{\alpha'\sigma'}P\big[\binom{n_{\rm L\uparrow},\, n_{\rm R\uparrow}}{n_{\rm L\downarrow},\, n_{\rm R\downarrow}}, t\big]$. Using the spin-resolved master equation (4), one finds

$$\begin{aligned}\frac{d}{dt}M^{\sigma\sigma'}_{\alpha\alpha'} = \frac{1}{2}e^2{\rm Tr}\big\{&\big[d^{\dagger}_{1\sigma}A^{(-)}_{\alpha\sigma} - A^{(+)}_{\alpha\sigma}d^{\dagger}_{1\sigma}\big]N^{\sigma'}_{\alpha'}(t) \\ &+ \big[d^{\dagger}_{1\sigma'}A^{(-)}_{\alpha'\sigma'} - A^{(+)}_{\alpha'\sigma'}d^{\dagger}_{1\sigma'}\big]N^{\sigma}_{\alpha}(t) \\ &+ \big[d^{\dagger}_{1\sigma}A^{(-)}_{\alpha\sigma} + A^{(+)}_{\alpha\sigma}d^{\dagger}_{1\sigma}\big]\rho_{\rm st}\delta_{\alpha\alpha'}\delta_{\sigma\sigma'} + {\rm H.c.}\big\},\end{aligned} \tag{11}$$

where $N^{\sigma}_{\alpha}(t)$ can be found from Eq. (6), and $\rho_{\rm st}$ is the stationary solution of the master equation (8). Specially, the zero-frequency spin-resolved noise which is of most interest reads[17, 26, 31, 33]

$$S^{\sigma\sigma'}_{\alpha\alpha'} = 2\frac{d}{dt}\big[M^{\sigma\sigma'}_{\alpha\alpha'}(t) - \bar{I}^{\sigma}_{\alpha}\bar{I}^{\sigma'}_{\alpha'}t^2\big]\big|_{t\rightarrow\infty}. \tag{12}$$

So far we have outlined a compact formalism for spin-dependent transport through mesoscopic systems, based on the standard second–order Born–Markov approximation. This approach, which can be considered as a finite temperature and voltage extension of the "n"-resolved quantum Bloch–type equation proposed by Gurvitz and

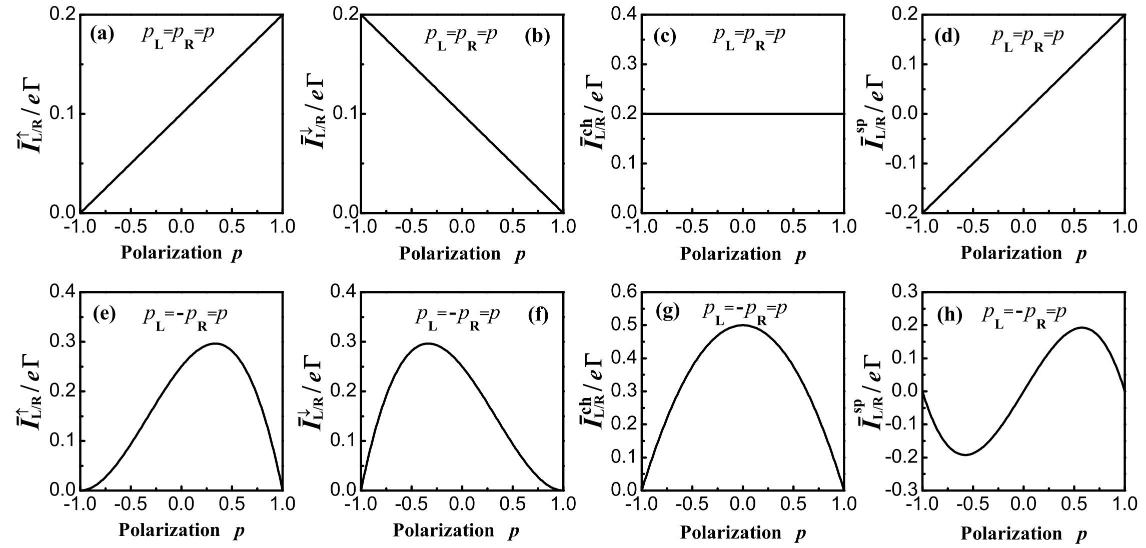

FIG. 2: Currents versus spin polarization p for parallel case (a)-(d), and antiparallel case (e)-(h). The coupling strengths are chosen to be $\Gamma_{\rm L} = \Gamma_{\rm R} = \Gamma$.

Prager[34], has the advantages of its simplicity of treating properly a broad range of dissipation, as well as its transparency in the involved dynamics and many-body interactions. As will be shown in the following, this approach can be efficiently used to study the spin-dependent transport phenomena, say, not only the spin-dependent currents, but also their noise properties.

IV. CURRENT CHARACTERISTICS

In the following, we consider two magnetic configurations. (i) Parallel case: $p_{\rm L} = p_{\rm R} = p$. The spin-dependent coupling strength can be expressed in terms of spin polarization as $\Gamma_{\alpha\uparrow/\downarrow} = \frac{1}{2}(1 \pm p)\Gamma_\alpha$ with α =L or R. (ii) Antiparallel case: $p_{\rm L} = -p_{\rm R} = p$. The strength of tunneling coupling thus reads $\Gamma_{{\rm L}\uparrow/\downarrow} = \frac{1}{2}(1 \pm p)\Gamma_{\rm L}$, and $\Gamma_{{\rm R}\uparrow/\downarrow} = \frac{1}{2}(1 \mp p)\Gamma_{\rm R}$, respectively.

In the regime of large bias voltage and low temperature, electrons only transport in one direction, say, from left electrode to the right one. The Fermi functions relevant to the transport processes can be approximated by either one or zero. Then simple expressions for the stationary spin-dependent currents, as well as the total charge and spin currents are available, as listed in table I. Numerical results for the currents are presented in Fig. 2 as a function of spin polarization p. The main features found here are summarized as follows: (i) there exists a symmetry relation between $\bar{I}^{\uparrow}_{\rm L/R}$ and $\bar{I}^{\downarrow}_{\rm L/R}$, which makes us only need to consider one of them; (ii) the total charge currents $\bar{I}^{\rm ch}_{\rm L/R}$ are symmetric about the axis $p = 0$; and (iii) the total spin currents $\bar{I}^{\rm sp}_{\rm L/R}$ are odd functions of p. Detailed features of the currents in both parallel and antiparallel cases are presented in the following.

The results for the parallel configuration are shown in Fig. 2(a)-(d). As the polarization of the FM electrodes is gradually altered from $p = -1$ to $p = 1$, the rate of tunneling a spin-up (spin-down) electron is increased (reduced). The spin-up (spin-down) current increases (decreases) linearly with the spin polarization p, as shown in Fig. 2(a) and (b). Thus the total charge current, which is the sum of these two current, is constant [see Fig. 2(c)]. The total spin current, being the difference of the two currents, therefore increases linearly with the polarization p, as displayed in Fig. 2(d).

For the antiparallel case, the magnetization directions of the two electrodes are opposite to each other. The spin currents vanish as the polarization $p \to \pm 1$. Let us consider, for instance, the spin-up current, which can be readily expressed as $\bar{I}^{\uparrow}_{\rm L} = \Gamma_{{\rm L}\uparrow}\rho_0$ with ρ_0 the probability of the coupled dot being empty. As the polarization p changes from -1 to 1, the probability ρ_0 first increases from zero to its maximum value at $p = 0$, and then decreases to zero, while the rate of tunneling a spin-up electron $\Gamma_{{\rm L}\uparrow}$ increases linearly. This leads to the unique feature of the spin-up current, as shown in Fig. 2(e). The overall structure of the total charge and spin currents, as displayed in Fig. 2(c) and (d), can be understand in terms of the individual spin currents.

Remarkably, in both parallel and antiparallel configurations all the currents are independent of the level mismatch $\Delta = E_1 - E_2$ and the interdot coupling strength Ω. Hereafter, by investigating the spin-resolved noises, we explore in detail the effect of interdot coupling, as well as the interplay between Coulomb correlations and the spin polarization of the FM electrodes.

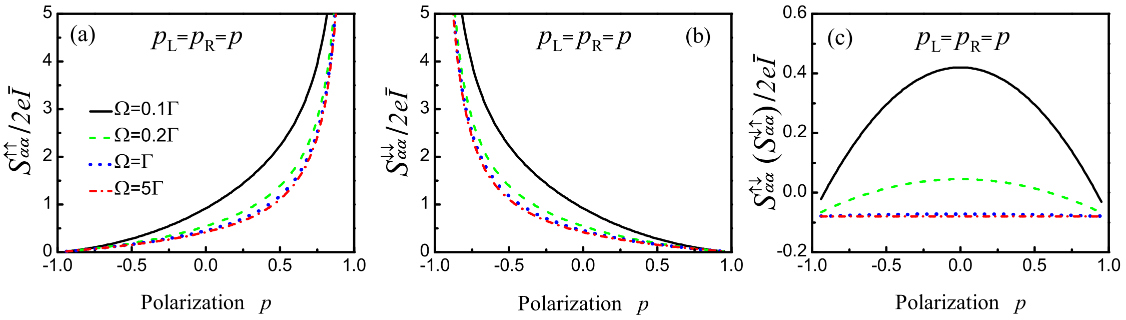

FIG. 3: Self spin correlation noises in parallel configuration for different interdot couplings: $\Omega = 0.1\Gamma$ (solid curve), $\Omega = 0.2\Gamma$ (dashed curve), $\Omega = \Gamma$ (dotted curves), and $\Omega = 5\Gamma$ (dash-dotted curve). Here we choose $\Gamma_{\rm L} = \Gamma_{\rm R} = \Gamma$, $\Delta = 0$.

V. NOISE CHARACTERISTICS

In this section, instead of using the circuit noise[25, 35, 36], we will investigate various fluctuations of spin currents through left or right junction, i.e. the auto-correlations $S_{\alpha\alpha}^{\sigma\sigma'}$ with α = L or R. For the cross-correlations, they simply satisfy the relation $S_{\rm LR}^{\sigma\sigma'} = -S_{\rm LL}^{\sigma\sigma'} = -S_{\rm RR}^{\sigma\sigma'}$ in the present two-terminal case, as we have checked. It should be noted that for a three-terminal structure such a simple relation generally does not hold (see, for instances, [37–39]).

A. Self spin correlation shot noise

The numerical results for self-correlation noises in the parallel and antiparallel cases are displayed in Fig. 3(a)-(b) and Fig. 4(a)-(b), respectively. There is a symmetry between $S_{\alpha\alpha}^{\uparrow\uparrow}$ and $S_{\alpha\alpha}^{\downarrow\downarrow}$ with respect to the spin polarization, i.e. Fig. 3(a) versus (b) and Fig. 4(a) versus (b). Therefore, it needs only to consider either $S_{\alpha\alpha}^{\uparrow\uparrow}$ or $S_{\alpha\alpha}^{\downarrow\downarrow}$.

Let us first consider the parallel case. For $S_{\alpha\alpha}^{\uparrow\uparrow}$ in Fig. 3(a), it increases monotonically with the polarization p, but decreases as the interdot coupling strength Ω grows. Remarkably, we observe a strong super-Poisson behavior. This novel behavior can be understood in terms of the so-called *dynamical spin blockade* mechanism[26, 37–39]. The Coulomb interaction prevents a double occupancy of the coupled dots, there will be competition between tunneling events for spin-up and spin-down electrons. The characteristic time for these two processes, due to polarization, is unequal: there is fast tunneling of spin-up electrons and slow tunneling of spin-down electrons through the system. The spin-down electron, which spends a long time on the dot, blocks the fast tunneling of the spin-up electrons. Eventually, for a large value of polarization, a mechanism of *fast-to-slow channels* is developed, which leads to an effective bunching of tunneling events and, consequently, to the supper-Poissonian shot noise.

Note that a strong Coulomb interaction is essential to the bunching behavior of tunneling events, otherwise the spin-up and spin-down electrons will transport through the system independently, and consequently, the noise remains sub-Poissonian[12]. The super-Poissonian noise can be realized as long as the electrodes are properly and sufficiently polarized. This finding is different from the double dots coupled in serial[26], where a strong interdot coupling is required for the super-Poissonian noise.

For the antiparallel alignment, the self-correlations turn out to be quite different, as shown in Fig. 4(a)-(b), Take again $S_{\alpha\alpha}^{\uparrow\uparrow}$ for illustration. If the left electrode is fully spin-down polarized, tunneling of spin-up electrons are suppressed, and thus $S_{\alpha\alpha}^{\uparrow\uparrow}$ vanishes as $p \to -1$. In the opposite limit of $p \to 1$, a spin-up electron which has tunneled from the left electrode into the coupled dots will stay there for a long time as the tunneling rate $\Gamma_{\rm R\uparrow}$ is greatly reduced. The tunneling events are thus uncorrelated, and the self spin correlation is Poisson, i.e. $S_{\alpha\alpha}^{\uparrow\uparrow} = 1$. In a wide range in between, the noise is very sensitive to the interdot coupling strength. For weak interdot coupling, as shown by solid curve in Fig. 4(a) for $\Omega = 0.1\Gamma$, a super-Poissonian noise is developed. Different from the parallel case, here, the so-called *dynamic charge blockade*[20, 40–45] is the dominant mechanism responsible for the super-Poissonian noise.Electron transport through the direct path (L→QD1 →R) has a fast characteristic time $\sim \Gamma_{\rm L/R}^{-1}$, while tunneling through the indirect path (L→QD1→DQ2→ QD1→R) has a slow characteristic time $\sim \Omega^{-1}$. In the limit where the DDCB prevent a double occupancy of the coupled dots, a competition between these two paths is developed. The slow flowing of electrons through the indirect path modulates electron transport through the direct path, which leads to a bunching of tunneling events, and finally to the super-Poissonian noise of $S_{\alpha\alpha}^{\uparrow\uparrow}$.

In this case, both DDCB and a weak interdot coupling are essential to the super-Poissonian noise. If the interdot coupling strength is enhanced, the characteristic time of electron tunneling through the indirect path would increase, and the competition mechanism is spoiled. Consequently, the self-correlation noise is sub-Poisson, as shown respectively, by dashed ($\Omega = 0.2\Gamma$),

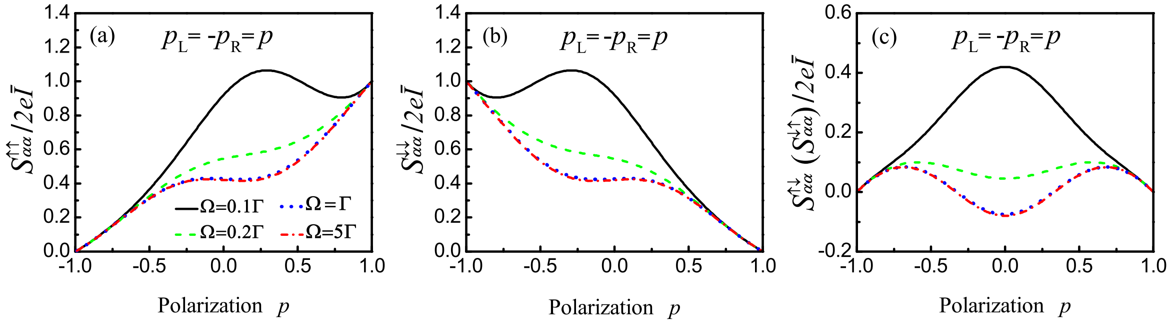

FIG. 4: Self spin correlation shot noises in antiparallel configuration for different interdot couplings: $\Omega = 0.1\Gamma$ (solid curve), $\Omega = 0.2\Gamma$ (dashed curve), $\Omega = \Gamma$ (dotted curves), and $\Omega = 5\Gamma$ (dash-dotted curve). Other parameters are the same as in Fig. 3.

dotted ($\Omega = \Gamma$), and dash-dotted ($\Omega = 5\Gamma$) curves in Fig. 4(a) and (b).

B. Mutual spin correlation shot noise

We now turn to the discussion of mutual spin correlation shot noise, i.e. $S^{\uparrow\downarrow}_{\alpha\alpha}$ or $S^{\uparrow\downarrow}_{\alpha\alpha}$. They simply satisfy the relation $S^{\uparrow\downarrow}_{\alpha\alpha} = S^{\uparrow\downarrow}_{\alpha\alpha}$. The numerical results are displayed in Fig. 3(c) and Fig. 4(c), for the parallel and antiparallel cases, respectively. In both cases, the mutual correlations are symmetric to the polarization.

For the parallel case, simple expression for the mutual correlation is available

$$S^{\uparrow\downarrow}_{\alpha\alpha} = S^{\downarrow\uparrow}_{\alpha\alpha} = 2e\bar{I}\left[\frac{(1-p^2)\Gamma_L^2\Gamma_R^2}{2(4\Gamma_L+\Gamma_R)^2\Omega^2} - \frac{2\Gamma_L\Gamma_R}{(4\Gamma_L+\Gamma_R)^2}\right]. \tag{13}$$

The first part gives a positive contribution, while the second term shows reduction effect. It implies that the spin-up and spin-down currents may be either positively or negatively correlated, depending on the polarization and interdot coupling strength. For strongly coupled dots, the mutual spin correlation is *fully negative*, as shown by dotted ($\Omega = \Gamma$) and dash-dotted ($\Omega = 5\Gamma$) curves in Fig. 3(c). However, if the two dots are weakly coupled to each other, the mutual correlation clearly demonstrates its sensitivity to the spin polarization, as displayed by solid ($\Omega = 0.1\Gamma$) and dashed ($\Omega = 0.2\Gamma$)curves in Fig. 3(c). Negative mutual correlation is found if the electrodes are sufficiently polarized, but positive correlation can be formed provided the electrodes are weakly or moderately polarized.

The numerical results of the antiparallel case are displayed in Fig. 4(c). For sufficiently polarized electrodes, i.e. $p \to \pm 1$, both spin-up and spin-down currents are greatly suppressed, and thus the mutual correlation vanishes. For weak interdot coupling, the mutual correlation is positive definite, as shown by the solid ($\Omega = 0.1\Gamma$) and dashed ($\Omega = 0.2\Gamma$) curves in Fig. 4(c). As interdot coupling strength increases, the mutual correlation may be either positive or negative, depending on the degree of spin polarization in the electrodes. That is, for sufficient polarization, the spin-up and spin-down currents are positively correlated, while negative mutual correlation can appear provided the electrodes are weakly spin polarized.

In concluding this subsection, we note that the super-Poissonian self spin correlation does not necessarily imply a positive mutual correlation, as shown by the dashed and dash-dotted curves in Fig. 3(c) for the parallel case, where the spin-up and spin-down currents are negatively correlated. Also, the sub-Poissonain self spin correlation and the negative mutual correlation does not have a one-to-one correspondence, as displayed by the dashed curve in Fig. 4(c), where the mutual correlation is fully positive.

C. Total charge and spin current noises

The total charge and spin current noises are readily obtained via proper combination of those components of the spin-resolved noises, according to Eqs. (9a) and (9b). The results for the parallel case are displayed in Fig. 5, and those for the antiparallel case are shown in Fig. 6. Here, most features such as the sub-Poisson and super-Poisson behaviors can be understood in terms of the above interpretation to the partial spin-resolved noises.

To complete this section, we consider all kinds of noises discussed above in the limit of $p = 0$. In this unpolarized situation, simple analytic results can be obtained. The self and mutual spin correlations read respectively,

$$S^{\uparrow\uparrow}_{\alpha\alpha} = S^{\downarrow\downarrow}_{\alpha\alpha} = e\bar{I}\left[1 - \frac{4\Gamma_L\Gamma_R}{4\Gamma_L+\Gamma_R} + \frac{\Gamma_L^2\Gamma_R^2}{(4\Gamma_L+\Gamma_R)^2\Omega^2}\right], \tag{14a}$$

$$S^{\uparrow\downarrow}_{\alpha\alpha} = S^{\downarrow\uparrow}_{\alpha\alpha} = e\bar{I}\left[\frac{\Gamma_L^2\Gamma_R^2}{(4\Gamma_L+\Gamma_R)^2\Omega^2} - \frac{4\Gamma_L\Gamma_R}{4\Gamma_L+\Gamma_R}\right]. \tag{14b}$$

The total charge and spin noises are thus obtained via Eq. (9),

$$S^{\rm ch}_{\alpha\alpha} = 2e\bar{I}\left[1 - \frac{8\Gamma_L\Gamma_R}{4\Gamma_L+\Gamma_R} + \frac{2\Gamma_L^2\Gamma_R^2}{(4\Gamma_L+\Gamma_R)^2\Omega^2}\right], \tag{15a}$$

$$S^{\rm sp}_{\alpha\alpha} = 2e\bar{I}. \tag{15b}$$

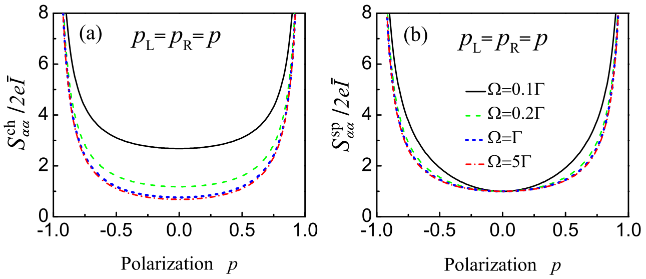

FIG. 5: Total charge and spin current noises in parallel configuration, obtained by appropriate combination of the spin-resolved noises as shown in Fig. 3 according to Eq. (9). Other plotting parameters are the same as in Fig. 3.

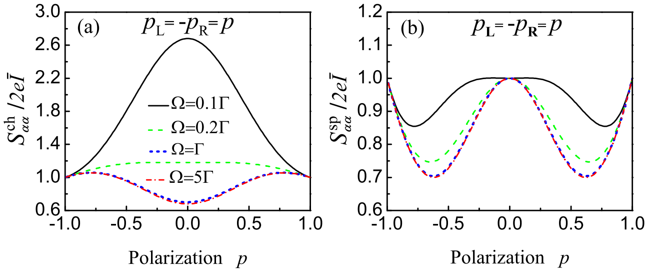

FIG. 6: Total charge and spin current noises in antiparallel configuration. Other plotting parameters are the same as in Fig. 3.

Remarkably, the total spin noise is Poissonian. This result can be interpreted in the following way. In presence of a strong Coulomb repulsion, each junction is sequentially crossed by elementary wave packets with well-defined but uncorrelated spins at $p = 0$. It implies very short time correlations therefore the total spin exhibits Poisson statistics[14].

VI. CONCLUSION

To summarize, based on the spin-resolved quantum master equation, we investigated the spin-dependent transport through T-shaped double quantum dots which is connected with ferromagnetic electrodes. The modulation of the interdot coupling, as well as the interplay between Coulomb interactions and spin polarization in the ferromagnetic electrodes give rise to a number of remarkable behaviors in the spin-resolved noises, such as super-Poissonian self spin correlations noises, as well as positive and negative mutual spin correlations. These unique noise features can serve as additional tool in experiments for revealing the intrinsic interdot coupling, as well as the involving Coulomb interactions.

Finally, we briefly discuss the measurement of spin current shot noise. It was shown in [46] that in hybrid ferromagnetic-normal metal structures, the spin current noise exerts a fluctuating spin torque on the magnetization vector, which causes an observable magnetization noise. By measuring this magnetization noise, which has been realized experimentally[47], one then obtains the spin current noise.

Acknowledgments

Support from the National Natural Science Foundation of China (10904128), Zhejiang Provincial Natural Science Foundation (Y6100171 and Y6110467) is gratefully acknowledged.

[1] G. A. Prinz, Science **282**, 1660 (1998).
[2] S. A. Wolf, D. D. Awschalom, R. A. Buhrman, J. M. Daughton, S. von Motnár, M. L. Roukes, A. Y. Chtchelkanova, and D. M. Treger, Science **294**, 1488 (2001).
[3] I. Žutić, J. Fabian, and S. D. Sarma, Rev. Mod. Phys. **76**, 323 (2004).
[4] F. J. Jedema, A. T. Filip, and B. J. van Wees, Nature **410**, 345 (2001).
[5] F. J. Jedema, H. B. Heersche, A. T. Filip, J. J. A. Baselmans, and B. J. van Wees, Nature **416**, 713 (2002).
[6] D. D. Awschalom, D. Loss, and N. Samarth, *Semiconductor spintronics and quantum computation* (Springer, Berlin, 2002).
[7] A. Brataas, Y. Tserkovnyak, G. E. W. Bauer, and B. I. Halperin, Phys. Rev. B **66**, 060404 (2002).
[8] B. Wang, J. Wang, and H. Guo, Phys. Rev. B **67**, 092408 (2003).
[9] P. Sharma and C. Chamon, Phys. Rev. Lett. **87**, 096401 (2001).
[10] E. R. Mucciolo, C. Chamon, and C. M. Marcus, Phys. Rev. Lett. **89**, 146802 (2002).
[11] Q.-F. Sun, H. Guo, and J. Wang, Phys. Rev. Lett. **90**, 258301 (2003).
[12] Y. M. Blanter and M. Büttiker, Phys. Rep. **336**, 1 (2000).
[13] Y. V. Nazarov, *Quantum Noise in Mesoscopic Physics* (Kluwer, Dordrecht, 2003).
[14] O. Sauret and D. Feinberg, Phys. Rev. Lett. **92**, 106601 (2004).
[15] B. Wang, J. Wang, and H. Guo, Phys. Rev. B **69**, 153301 (2004).
[16] I. Djuric, B. Dong, and H. L. Cui, J. Appl. Phys. **99**, 063710 (2006).
[17] B. Dong, H. L. Cui, and X. L. Lei, Phys. Rev. Lett. **94**, 066601 (2005).
[18] T.-S. Kimand and S. Hershfield, Phys. Rev. B **63**, 245326 (2001).
[19] P. S. Cornaglia and D. R. Grempel, Phys. Rev. B **71**, 075305 (2005).
[20] I. Djuric, B. Dong, and H. L. Cui, Appl. Phys. Lett. **87**, 032105 (2005).

[21] S. S. Safonov, A. K. Savchenko, D. A. Bagrets, O. N. Jouravlev, Y. V. Nazarov, E. H. Linfield, and D. A. Ritchie, Phys. Rev. Lett. **91**, 136801 (2003).

[22] A. Nauen, F. Hohls, J. Könemann, and R. J. Haug, Phys. Rev. B **69**, 113316 (2004).

[23] X. Q. Li, J. Y. Luo, Y. G. Yang, P. Cui, and Y. J. Yan, Phys. Rev. B **71**, 205304 (2005).

[24] X. Q. Li, P. Cui, and Y. J. Yan, Phys. Rev. Lett. **94**, 066803 (2005).

[25] J. Y. Luo, X.-Q. Li, and Y. J. Yan, Phys. Rev. B **76**, 085325 (2007).

[26] J. Y. Luo, X.-Q. Li, and Y. J. Yan, J. Phys.: Cond. Matt. **20**, 345215 (2008).

[27] D. A. Papaconstantopoulos, *Handbook of the Band Structure of Elemental Solids* (Plenum Press, New York, 1986).

[28] K. Ono, D. G. Austing, Y. Tokura, and S. Tarucha, Science **297**, 1313 (2002).

[29] Y. J. Yan, Phys. Rev. A **58**, 2721 (1998).

[30] D. K. C. MacDonald, *Noise and Fluctuations: An Introduction* (Wiley, New York, 1962), ch. 2.2.1.

[31] C. Flindt, T. Novotný, and A.-P. Jauho, Physica E **29**, 411 (2005).

[32] D. Mozyrsky, L. Fedichkin, S. A. Gurvitz, and G. P. Berman, Phys. Rev. B **66**, 161313 (2002).

[33] B. Elattari and S. A. Gurvitz, Phys. Lett. A **292**, 289 (2002).

[34] S. A. Gurvitz and Y. S. Prager, Phys. Rev. B **53**, 15932 (1996).

[35] S. A. Gurvitz, D. Mozyrsky, and G. P. Berman, Phys. Rev. B **72**, 205341 (2005).

[36] R. Aguado and T. Brandes, Phys. Rev. Lett. **92**, 206601 (2004).

[37] D. A. Bagrets and Y. V. Nazarov, Phys. Rev. B **67**, 085316 (2003).

[38] A. Cottet, W. Belzig, and C. Bruder, Phys. Rev. B **70**, 115315 (2004).

[39] A. Cottet, W. Belzig, and C. Bruder, Phys. Rev. Lett. **92**, 206801 (2004).

[40] G. Kießlich, H. Sprekeler, and E. Schöll, Semicond. Sci. Technol. **19**, S37 (2004).

[41] A. Thielmann, M. H. Hettler, J. König, and G. Schön, Phys. Rev. B **71**, 045341 (2005).

[42] G. Kießlich, A. Wacker, and E. Schöll, Phys. Rev. B **68**, 125320 (2003).

[43] G. Kießlich, E. Schöll, T. Brandes, F. Hohls, and R. J. Haug, Phys. Rev. Lett. **99**, 206602 (2007).

[44] R. Sánchez, S. Kohler, P. Hänggi, and G. Platero, Phys. Rev. B **77**, 035409 (2008).

[45] F. Li, H. J. Jiao, J. Y. Luo, X.-Q. Li, and S. A. Gurvitz, arXiv:0812.0846 (2008).

[46] J. Foros, A. Brataas, Y. Tserkovnyak, and G. E. Bauer, Phys. Rev. Lett. **95**, 016601 (2005).

[47] M. Covington, M. AlHajDarwish, Y. Ding, N. J. Gokemeijer, and M. A. Seigler, Phys. Rev. B **69**, 184406 (2004).